Atmos. Chem. Phys. Discuss., doi:10.5194/acp-2016-421, 2016
Manuscript under review for journal Atmos. Chem. Phys.
Published: 13 July 2016

Atmospheric Chemistry and Physics Discussions

Surface Renewal as a Significant Mechanism for Dust Emission

Jie Zhang[1,2], Zhenjiao Teng[2], Ning Huang[1,2], Lei Guo[2] , Yaping Shao[3]

[1]Key Laboratory of Mechanics on Disaster and Environment in Western China, Lanzhou University, 730000 Lanzhou, China
[2]School of Civil Engineering and Mechanics, Lanzhou University, 730000 Lanzhou, China
[3]Institute for Geophysics and Meteorology, University of Cologne, 50937 Cologne, Germany

Correspondence to: N. Huang (huangn@lzu.edu.cn)

Abstract. Wind-tunnel experiments of dust emissions from different soil surfaces are carried out to better understand dust emission mechanisms. The effects of surface renewal on aerodynamic entrainment and saltation bombardment are analysed in detail, and the measurements are used to test published dust models. It is found that flow conditions, surface particle motions (saltation and creep), soil dust content and ground obstacles all strongly affect dust emission, causing dust emission rate to vary over orders of magnitude. Aerodynamic entrainment is highly effective, if dust supply is unlimited, as in the first 2-3 minutes of our wind-tunnel runs. While aerodynamic entrainment is suppressed by dust supply limit, surface renewal through the motion of surface particles is found to be an effective pathway to remove the supply limit. Surface renewal is also found to be important to the efficiency of saltation bombardment. We demonstrate that surface renewal is a significant mechanism affecting dust emission and recommend that this mechanism be included in future dust models.

Keywords: dust emission; surface renewal; aerodynamic entrainment; wind tunnel; supply limit

1. Introduction

Three dust emission mechanisms have been identified, including (1) aerodynamic entrainment; (2) saltation bombardment; and (3) aggregates disintegration (Shao, 2008; Kok et al., 2012; Újvári et al., 2016). In spite of much research effort, many questions remain unanswered in relation to the process of dust emission. For example, in most existing dust emission schemes, aerodynamic entrainment is assumed to be small and negligible. It is however questionable, to what extent and under what conditions this assumption is justified, because there is hardly any data which enable a rigorous comparison of aerodynamic entrainment from natural soil surfaces with the other dust emission mechanisms. For natural soils, dust emission is usually "supply limited" (Shao, 2008; Macpherson et al., 2008; Újvári et al., 2016), i.e., the emission is limited by the availability of free particles on the soil surface, rather than by the shear stress that wind exerts. However, “supply limit” is not a quantified term in published emission models, as little is known about its spatial and temporal variations. The argument for the neglect of aerodynamic entrainment is that dust particles have relatively large cohesive forces and are resistant to aerodynamic lift, and thus saltation bombardment and aggregates disintegration are the dominant mechanisms for dust emission (Greeley and Iversen, 1985; Shao et al., 1993). Researchers have noted there are obvious differences in dust emission from disturbed and undisturbed soils (Macpherson et al., 2008), which indicates that aerodynamic entrainment can play an important role if the supply of dust is less limited. Further, in existing dust models, the conditions of the surface

Atmos. Chem. Phys. Discuss., doi:10.5194/acp-2016-421, 2016
Manuscript under review for journal Atmos. Chem. Phys.
Published: 13 July 2016

Atmospheric Chemistry and Physics Discussions

subjected to erosion are assumed to be stationary. In reality, during an erosion event, surface self-disturbance occurs due to top soil removal and particle impact, i.e., a surface renewal process takes place, which in general enhances the supply of dust for aerodynamic entrainment. We argue that under the conditions of strong surface renewal, aerodynamic entrainment may be a significant mechanism for dust emission.

In this work, we simulate three typical landforms in a wind-tunnel experiment, namely, a farmland surface, a desert surface and a loess surface (see Section 3 for details). We then sought to quantify the contributions of three dust emission mechanisms to the total dust flux for the different landforms. Using the wind-tunnel observations, we demonstrated that supply limit of free dust is the primary factor which suppresses aerodynamic entrainment, but surface renewal through saltation and creep provides an important pathway to enhance free dust supply for aerodynamic entrainment. Thus, for surfaces with strong renewal and sufficient free dust supply, aerodynamic entrainment becomes a non-negligible process for dust emission.

2. Model and Method

2.1 Aerodynamic Entrainment

Aerodynamic entrainment refers to direct dust uplifted from the surface into the atmosphere by aerodynamic forces. It has been suggested that the dust flux arising from aerodynamic entrainment is inconsequential, because aerodynamic lift force for small particles is in general small compared to inter-particle adhesion. Loosmore and Hunt (2000) suggested based on their wind-tunnel experiments that

$$F_a = 3.6\, u_*^3 \tag{1}$$

where F_a ($\mu g \cdot m^{-2} \cdot s^{-1}$) is dust emission flux due to aerodynamic entrainment and u_* ($m \cdot s^{-1}$) is friction velocity. However, inter-particle cohesive force is a stochastic variable, such that there always exists in nature a proportion of dust which is free, i.e., dust for which inter-particle cohesion is weak (Shao, 2008). Several studies have demonstrated that F_a is not always negligible (Kjelgaard et al., 2004; Macpherson et al., 2008; Klose and Shao, 2012; Sweeney and Mason, 2013), but the key factors which determine aerodynamic entrainment remain poorly understood. Moreover, Loosmore and Hunt (2000) conducted the wind tunnel experiments by using “Arizona Test Dust” (ISO-12103-1) to produce very smooth test beds. The investigation of dust emission caused by aerodynamic entrainment over natural and rough surfaces is still lacking.

2.2 Saltation Bombardment

Saltation bombardment is considered as the central mechanism of dust emission and has been extensively studied. Based on field experiments (Gillette, 1974, 1977 and 1981), Gillette & Passi (1988, GP88 hereafter) proposed an empirical formula for dust flux due to saltation bombardment, F_b, as a function of friction velocity

Atmos. Chem. Phys. Discuss., doi:10.5194/acp-2016-421, 2016
Manuscript under review for journal Atmos. Chem. Phys.
Published: 13 July 2016

Atmospheric Chemistry and Physics Discussions

$$F_b = c \cdot u_*^4 (1 - \frac{u_{*t}}{u_*}) \quad (2)$$

where u_{*t} is threshold friction velocity and c an empirical constant. Marticorena and Bergametti (1995) suggested that F_b is dependent on streamwise saltation flux (Q), and soil content (η_c),

$$F_b = a_1 \, e^{a_2 \eta_c + a_3} \, Q \quad (3)$$

where a_1, a_2 and a_3 are empirical constants. Based on the wind-tunnel observations by Rice et al. (1996a, b) and Shao (1993, 1996), Lu & Shao (1999, LS99 hereafter) and Shao (2000, 2001) argued that a blasting saltator, upon its impact, causes a bombardment effect which results in dust emission. The latter authors derived an expression for dust emission by saltation

$$F = \frac{c_b g \eta \rho_b}{P} \left(1 + 14 u_* \sqrt{\frac{\rho_b}{P}}\right) Q \quad (4)$$

where c_b is a constant, g is gravitational acceleration, η is the mass fraction of dust inside the crater, ρ_b is the soil bulk density, P is the horizontal component of soil plastic pressure determined by soil property.

2.3 Aggregates Disintegration

Studies on aggregates disintegration are rare. Shao (2001) presented a dust emission model which accounts for both the effect of saltation bombardment and aggregates disintegration. This model, as simplified in Shao (2004, S04 hereafter), can be summarized as follows:

$$F = \sum_{i=1}^{I} F(d_i) \quad (5)$$

$$F(d_i) = \int_{d_1}^{d_2} F(d_i, d_s) p(d_s) \, \delta d_s \quad (6)$$

$$F(d_i, d_s) = c_y \eta_{fi} \left[(1 - \gamma) + \gamma \sigma_p\right] (1 + \sigma_m) \frac{g Q(d_s)}{u_*^2} \quad (7)$$

where F is total dust flux, d_i is the particle size of the ith bin out of the total I bins, d_s is the particle size of the saltator, d_1 and d_2 are the lower and upper limits of d_s, $p(d_s)$ is the particle size distribution of d_s, c_y is a dimensionless coefficient, η_{fi} is total dust fraction of the ith bin, $\gamma = \exp[-(u_* - u_{*t})^3]$ in which u_* is the friction velocity and u_{*t} is the threshold friction velocity, σ_p is the ratio of aggregated dust to free dust, σ_m is the mass ratio of ejectiles to saltators (i.e., bombardment efficiency) derived from the saltation model by Lu and Shao (1999), and $Q(d_s)$ is the flux of the saltators. Equation (5) sums the dust fluxes over all size bins and Equation (6) gives the dust flux of particles in the ith bin.

In the end, F is found to be proportional to $Q(d_s)$, but the proportionality depends on soil texture and soil plastic pressure. Further simplification indicates that at high soil plastic pressure (>3 × 10^5 Pa), σ_m becomes negligibly small (< 0.1) under normal wind conditions, and saltation bombardment diminishes to such an extent that aggregates disintegration prevails.

In this work, we consider the total dust flux, F, as the sum of contributions from the three individual mechanisms

Atmos. Chem. Phys. Discuss., doi:10.5194/acp-2016-421, 2016
Manuscript under review for journal Atmos. Chem. Phys.
Published: 13 July 2016

Atmospheric Chemistry and Physics Discussions

$$F = F_a + F_b + F_c \quad (8)$$

Our basic assumptions are as follows. Let the dust exposed on a bare soil surface be the available dust for emission. Then, the thoroughly disturbed soil possesses the maximum amount of available dust. As dust emission proceeds, supply limit occurs when the available dust falls below a critical level. We define the replenishment of available dust as surface renewal. Then, saltation and creep enable surface renewal in several ways: (1) remove particles on the surface to expose the underlying dust; (2) spear into the soil to dislodge the dust initially not available; and (3) blast onto aggregates and break them to release new surface dust. Surface renewal does not directly cause dust emission but recover surface available dust, which is the main difference from normal saltation bombardment mechanism.

3. Wind Tunnel Experiment

We conducted the experiments in the wind tunnel of Lanzhou University. This open-return blow-down low-speed wind tunnel is 22 m long with a cross section of 1.3 m wide and 1.45 m high. The operational wind speed can be adjusted in the range of 4-40 $m \cdot s^{-1}$. The wind tunnel has excellent performance in simulating atmospheric boundary-layer flows for near-surface wind environment studies. The detailed information of the wind tunnel could be found in Zhang et al. (2014).

3.1 Experimental Setup

The setup for the experiments is as shown in Figure 1. Roughness elements are placed 6 m upstream the working section to initiate a turbulent boundary layer. Their heights are adjusted to ensure a logarithmic wind profile (up to 20 cm above ground) in the downstream measurement area under all applied flow speeds. A test surface is located immediately downstream the roughness elements, which is 9 m long, 1 m wide and 5 cm deep and is paved with a soil. For measuring saltation, a sand trap is installed 8 m downstream from the frontal edge of the test surface. Two dust concentration probes are placed at 7 cm and 14 cm above the surface, each connected to a 1.109 Grimm aerosol spectrometer (Grimm Aerosol Technik GmbH & Co. KG). A Pitot tube is anchored to an adjustable frame for measuring the profile of the flow speed at 10 sampling points at 10, 15, 20, 30, 50, 70, 100, 130, 160 and 200 mm above the surface.

A farmland soil collected from Minqin of Gansu Province of China (natural soil hereafter) and natural sand collected from the Tengger Desert (natural sand hereafter) are used for the preparation of the test surfaces. Three land surfaces are tested as shown in Figure 1. In Setting 1 (S1), the natural soil is used for the entire test bed. In Setting 2 (S2), the first 4 m of the test bed is paved with the natural sand ahead of 5 m natural soil, to examine how enhanced saltation affects dust emission with respect to S1. In Setting 3 (S3), the natural soil is first sieved with a 20 mesh (841 μm) sieve (sieved soil hereafter) and then paved to simulate sieved soil. In this setting, the lumpy aggregates are removed. S1 represents a farmland surface, S2 a desert-edge surface and S3 a loess surface.

Atmos. Chem. Phys. Discuss., doi:10.5194/acp-2016-421, 2016
Manuscript under review for journal Atmos. Chem. Phys.
Published: 13 July 2016

Atmospheric Chemistry and Physics Discussions

3.2 Instruments and Measurements

By regression of the Prandtl–von Kármán equation

$$u(z) = \frac{u_*}{\kappa} ln\left(\frac{z}{z_0}\right) \quad (9)$$

to the Pitot-tube measurements, the friction velocity, u_*, and surface roughness, z_0, are calculated. In Equation (9), z is height, $u(z)$ is the mean flow velocity at height z and κ=0.4 is the von Kármán constant.

The particle size distributions of the natural soil, natural sand and sieved soil were analysed by using a Microtrac S3500 Laser Diffractometer (Microtrac, Montgomeryville, PA, USA) and approximated with an overlay of multiple normal distributions

$$d \times p(d) = \sum_{j=1}^{N} \frac{W_j}{\sqrt{2\pi}\sigma_j} exp[-\frac{(lnd-lnD_j)^2}{2\sigma_j^2}] \quad (10)$$

where N is the number of log-normal distribution modes ($N \leq 4$), W_j is the weight of the jth normal distribution, D_j and σ_j are the parameters in the jth normal distribution. The particle size distribution of minimally disturbed soil $p_m(d)$ and fully disturbed soil $p_f(d)$ are measured similarly to Shao et al. (2011). The soil sample is dispersed in water and the resulting particle size distribution taken as $p_m(d)$. The soil is firstly ground in a mortar and then be dispersed in 2% sodium hexametaphosphate to prepare the measurement for $p_f(d)$. The sonication step in Shao et al. (2011) is replaced with grinding in measuring $p_f(d)$ because sonication has incomparably stronger power than the particle collision during saltation.

The saltation flux is measured using a sand trap adapted from the WITSEG sampler designed by Dong et al. (2003). Facing the wind stream are 38 stacked collectors (2 cm × 2 cm opening), each of which collects sand to its chamber. The streamwise saltation flux, Q, is then determined by weighing the sand in the chambers after each run:

$$Q = \sum_{i=1}^{38} q_i \Delta h_i \quad (11)$$

$$q_i = \frac{m_i}{t_s A_i} \quad (12)$$

where Δh_i is the vertical size if inlet for collector i mounted at height h_i above the surface, q_i is the saltation flux at h_i, m_i is the mass of sand collected at h_i, t_s is the time duration of sand collection and A_i is the inlet area of the collector.

Once emitted, dust is transported vertically by turbulent diffusion. Assuming steady state and horizontal homogeneity, the vertical diffusive flux is equal to dust emission flux, which can be calculated using the gradient method. In our experiments, dust concentration, C, is measured at z_1 = 7 cm and z_2 = 14 cm above the surface, and thus dust emission rate can be calculated as

$$F = -K_p \frac{C(z_2)-C(z_1)}{z_2-z_1} \quad (13)$$

Atmos. Chem. Phys. Discuss., doi:10.5194/acp-2016-421, 2016
Manuscript under review for journal Atmos. Chem. Phys.
Published: 13 July 2016

Atmospheric Chemistry and Physics Discussions

where K_p is the turbulent diffusion coefficient for dust particles, which can be approximated as

$$K_p = K_m = u_* l \quad (14)$$

with l being the mixing length, taken here as $\kappa(z_1+z_2)/2$.

3.3 Procedures of Wind-tunnel Experiments

The wind-tunnel experiments are carried out according to the settings given in Table 1 and the following procedures:

1. Prepare soil and pave test bed as shown in Figure 1;
2. Set up instruments as shown in Figure 1;
3. Set fan to target flow speed; measure dust concentration and wind speed over 10 minutes; end run early if test bed is blown bare or sand chambers are filled;
4. Turn off fan; record time duration for saltator collection; weigh mass of collected saltators; save dust concentration data measured with aerosol spectrometer;
5. Restart fan set to the same target speed as Step 3, and measure wind profile;
6. Remove paved soil (soil must not be reused because emission has changed dust content). Start over from Step 1 for next run.

4. Results and Analysis

4.1 Particle Size Distribution of Source Materials

The particle size distributions of the natural soil, natural sand and sieved soil are shown in Figure 2. The dots represent the measured values, while the lines represent Equation (10) fitted to the measurements (see Table 2 for fitting parameters). For the natural sand, the fraction of particles in the size range of 10-200 μm increased due to grinding, while for the natural soil and sieved soil in the 1-10 μm and 30-60 μm size ranges.

The natural soil contained many lumps (diameter in centimetre scale) that can be easily broken by external impact or abrasion. These lumps disperse in water and thus the similarity in $p_m(d)$ between the natural and sieved soils does not reflect the existence of the large lumps in the natural soil. However, the lumps may significantly influence dust emission by causing spatial shear stress variations and by sheltering the surface from erosion. It was also found that the soil lumps were easily destroyed during the sieving process and the characterization of large soil lumps remains a problem to be better solved in future research.

Atmos. Chem. Phys. Discuss., doi:10.5194/acp-2016-421, 2016
Manuscript under review for journal Atmos. Chem. Phys.
Published: 13 July 2016

Atmospheric Chemistry and Physics Discussions

4.2 Saltation Bombardment

The measured and predicted streamwise saltation fluxes are shown in Figure 3. For given friction velocity, the sieved soil (S3) has slightly higher saltation flux than the natural soil under sand bombardment (S2), but both are much higher than the natural soil (S1). The Owen (1964) saltation model (dotted curve in Figure 3)

$$Q = c_0 \frac{\rho}{g} u_*^3 \left(1 - \frac{u_{*t}^2}{u_*^2}\right) \quad (15)$$

fits well to the measured fluxes, where c_0 is the Owen coefficient and u_{*t} is the threshold friction velocity and ρ is air density. The Owen saltation model is best applied to describe the saltation of uniform particle sizes, for which the two important parameters, namely, c_0 and u_{*t}, are well defined. For a surface with mixed particles, u_{*t} can be interpreted as a mean threshold friction velocity over a particle size range and c_0 reflects the fraction of effective saltators, namely, grains available for saltation at a given friction velocity, u_*. The fraction of effective saltators depends on the size distribution of the surface soil, the threshold friction velocity for each particle size bin and the spatial variation of u_*.

In S1, the presence of soil lumps not only increased significantly the threshold friction velocity compared with the sieved soil in S3, but also reduced the fraction of effective saltators as manifested in the low c_0 values. In S2, the saltators were mainly the natural sand particles which have a higher threshold friction velocity than the sieved soil. Because the natural sand has a narrow size range, the fraction of effective saltators was high once u_* exceeded u_{*t}, as seen in the high c_0 value.

The above fitting is straightforward and gives reasonable results except for the cases when the friction velocity is close to the threshold friction velocity and the Owen coefficient is mainly dependent on the fraction of effective saltators. To further verify the prediction of the regression function, we calculated the saltation fluxes for different particle size bin and their integral over the size bins as follows:

$$Q = \int_{d_1}^{d_2} Q(d_s)\, p(d_s) \delta d \quad (16)$$

$$Q(d_s) = c_0 \frac{\rho}{g} u_*^3 \left(1 - \frac{u_{*t}^2(d_s)}{u_*^2}\right) \quad (17)$$

$$c_0 = 0.25 + \frac{v_t}{3u_*} \quad (18)$$

$$u_{*t}(d_s) = \sqrt{A_n(\sigma_\varphi g d_s + \frac{r}{\rho d_s})} \quad (19)$$

where $p(d_s)$ is the measured soil size distribution (Figure 2), σ_φ the particle to air density ratio, v_t the particle terminal velocity and A_n and r the regression parameters (Shao and Lu, 2000). It is seen in Figure 3 that the above method gives a more accurate estimate of Q than Equation (15). Note that the key difference here is an improved estimate of u_{*t} for different particle size groups, as the values of A_n and r differ for different soils.

Atmos. Chem. Phys. Discuss., doi:10.5194/acp-2016-421, 2016
Manuscript under review for journal Atmos. Chem. Phys.
Published: 13 July 2016

Atmospheric Chemistry and Physics Discussions

4.3. Vertical Dust Flux

Vertical dust fluxes can be calculated with Equations (13) and (14) using the measured dust concentrations at the levels of 7 cm and 14 cm. In this study, dust is defined as particles smaller than 15 μm, such that the requirements for using the gradient method are satisfied (Shao et al., 2011). It can be seen from Figure 4 that for S1, dust emission has an initial sharp increase followed by a rapid decline (Fig. 4a). The same phenomenon has been reported in earlier studies and is considered to be characteristic of aerodynamic entrainment under limited supply (Shao, 1993; Loosmore and Hunt, 2000). In our experiments, paving the test bed causes mechanical disturbances to the soil. Thus, at the beginning of the run, the amount of free dust available for aerodynamic entrainment was close to the maximum for the given soil. As the dust emission continued, the amount of available free dust was gradually depleted and eventually exhausted. After about three minutes, dust emission was mainly attributed to weak saltation bombardment (Fig. 4). We therefore separate the time series into the two sections of 0-3 min and 3-10 min. The dust flux averaged over the 0-3 min section, $F_{0\text{-}3\ min}$, is the dust emission due to both aerodynamic entrainment and saltation bombardment with unlimited dust supply. The dust flux averaged over the 3-10 min section, $F_{3\text{-}10\ min}$ (F_b), is the dust emission due to saltation bombardment under limited dust supply (here, the effect of aggregates disintegration is not discussed individually and the related contribution is involved in F_b). The difference $F_{0\text{-}3\ min}$ - $F_{3\text{-}10\ min}$ (F_a) is then considered the dust emission due to aerodynamic entrainment under unlimited dust supply (Fig. 5).

In contrast, S2 and S3 did not show such a remarkable decrease of dust flux after the initial phase, probably due to the intensive saltation (see Fig. 2) which timely replenished the dust supply. Also for S2 and S3, we consider the dust flux averaged over the period of 3 to 10 minute as the dust emission for the corresponding surfaces (Fig. 5).

The results of Loosmore & Hunt (2000) and Macpherson et al. (2008), denoted as LH2000 and MP2008, respectively, are also shown in Figure 5. It can be seen that dust fluxes increase with friction velocity by following a power function, but the results for the three surfaces differ by several orders of magnitudes. S1 resembled the unperturbed surface in MP2008, whereas S2 and S3 resembled the renewed surface in MP2008, indicating that the soil surface was indeed renewed in S2 by external sand bombardment and in S3 by spontaneous saltation and creep of big particles. The flux in S2 was about one order of magnitude greater than that in S1 because the former had stronger saltation bombardment. The flux in S3 was another order of magnitude greater than that in S2 because of the higher content of effective surface dust. We also noted that the dust flux of S1 under unlimited supply was far greater than that in LH2000 (Fig. 5) and the maximum flux ($F_{a|max}$, which is about three times the average flux) even exceeded the dust flux due to strong saltation bombardment in S2. This should be due to the uneven distribution of surface shear force over the coarse soil surface in S1. Thus, the flow conditions, surface particle motion, dust availability, surface roughness and other factors can all cause dust fluxes to differ by orders of magnitudes.

Regression analysis shows that in S1, the natural soil with weak saltation bombardment had a dust flux proportional to u_*^4, in agreement with Gillette and Passi (1988). The introduction of saltation bombardment in S2 increased dust emission by one order of magnitude, with dust flux proportional to u_*^6. In S3, dust flux increased by two orders of magnitude compared to S1,

Atmos. Chem. Phys. Discuss., doi:10.5194/acp-2016-421, 2016
Manuscript under review for journal Atmos. Chem. Phys.
Published: 13 July 2016

Atmospheric Chemistry and Physics Discussions

with dust flux proportional to u_*^7. But under unlimited supply in S1, the dust flux was proportional to u_*^{10}. We note that with intensified surface renewal from S1 to S3, the relationship between dust flux and friction velocity increasingly resembled the aerodynamic entrainment under unlimited supply. An interpretation of this can be that strong saltation bombardment and creep enabled surface renewal, thus removing supply limit and maintaining dust emission at a high level. From this point of view, dust emission can be considered to be mainly driven by aerodynamic entrainment, whereas saltation and creep are responsible for surface renewal which restores the availability of dust for emission. In general, dust emission can be seen as the result of restricted aerodynamic entrainment.

4.4. Bombardment Efficiency

Figure 6 shows how bombardment efficiency, $\eta = F/Q$, (Gillette, 1979; Marticorena and Bergametti, 1995; Shao, 2008; Macpherson et al., 2008) varies with friction velocity, u_*. Previous studies suggested that dust emission is mainly due to saltation bombardment and for a given surface η appears to be a relatively stable constant (Marticorena and Bergametti, 1995; Houser and Nickling, 2001). Others found that η increases with u_* (Nickling et al., 1999; Kok et al., 2012) and this increase should be dependent on surface conditions (Shao, 2001). However, measurements are so far insufficient to verify this theory. In MP2008 (Macpherson et al., 2008), as the surface conditions were very complex, the measured bombardment efficiency scattered over a wide range of 4 orders of magnitude and did not show a fixed relationship with friction velocity. The bombardment efficiencies we measured are shown in Figure 6. It is observed that for all settings, η ranged between 2.0 and 3.0×10^{-4} m^{-1} at small u_*. However, it behaved differently as u_* increased. In S1, it decreased exponentially with u_*. This decrease cannot be explained using the existing dust emission modes (Lu and Shao, 1999; Shao, 2001, 2004). It is likely that as saltation bombardment was weak in S1 and could only lift the dust in a thin soil layer. Once the dust in this thin layer was depleted, the surface became dust supply limit. The bombardment efficiency of S2 was slightly higher than in S1 at low friction velocity. Although both surface types are natural soil, the moving sand particles may be more effective in the bombardment process (or aggregates disintegration process), and thus enhance the bombardment efficiency. In S2, with the increase of u_*, the large amount of saltators from the upstream may have buried the dust on the surface of the test bed and changed its properties, thus leading to the decline in bombardment efficiency similar to S1. As u_* further increased, the sand particles would not settle on the test bed, but continue to strike the surface and expose more dust to air, and thus increasing the bombardment efficiency. Hence, the degree of surface renewal significantly affects the bombardment efficiency. In S3, the available dust content is high and the bombardment efficiency is much higher than that in S1 and S2. The sieved soil used in S3, free from the sheltering of the lumps, is very mobile. Thus, as wind speed increased, the sieved soil particles undertook strong bombardment over the surface and enhanced surface renewal. This allowed an unlimited dust supply to maintain the bombardment efficiency. But even this does not seem to explain the increase of η with exponent of u_* (blue line in Fig. 6). While the decline of η with u_* in S1 and the preceding stage of S2 may be due to the inadequate replenishment of dust supply, the increase of η with u_* in S3 and the last stage of S2 must be due to the contribution of aerodynamic entrainment. Figure 5 also shows that the power of u_* is 7 in S3, which is close to the model flux equation of aerodynamic

Atmos. Chem. Phys. Discuss., doi:10.5194/acp-2016-421, 2016
Manuscript under review for journal Atmos. Chem. Phys.
Published: 13 July 2016

Atmospheric Chemistry and Physics Discussions

entrainment (F_a). This implies that the strong saltation bombardment enabled surface renewal and dust supply to maintain saltation bombardment efficiency. If the surface renewal is inadequate, then η decreases with u_*. In contrast, the saltation and creep generate sufficient surface renewal and hence dust supply, then η increases with u_*.

4.5. Comparison with Model Predictions

Figure 7 shows the averaged dust flux over the time interval from 3 to 10 min and the predictions using the models of GP88, LS99 and S04. As shown, the differences between the predictions of GP88 and the measured data near critical friction velocity are obviously bigger than the results of other two models for all three settings. That is caused by the indefinable empirical coefficient, c, for mixed-particle surfaces. In S1, dust emission occurred in the case of limited supply. Due to the neglect of the supply-limiting effect and of the variation of bombardment efficiency, all three models underestimated the dust flux at low friction velocity, but slightly overestimated at high friction velocity. For S2, all three models underestimated dust flux at low and high friction velocities but overestimated dust flux at intermediate level of friction velocity. At low u_* (just above u_{*t}), the saltating sand impacts on soil surface with relative high bombardment efficiency to cause dust emission. With the increase of u_*, the bombardment efficiency decreases because of changed surface property due to intrusive sand particles. At high u_*, wind was strong enough to move deposited sand particles and renewal surface. For the latter case, the performances of models are better. But, as all three models do not consider surface renewal and the consequent parametric change, the deviation of the predictions from the measurements naturally occurs. In S3, notable saltation and creep took place, which generated significant surface renewal. S04 appears to perform somewhat better than the others due to improved treatment for saltation bombardment and aggregates disintegration. Note that for the fitting of GP88 to the dust flux data (Figure 7), a very different u_{*t} was used than that for the fitting of the Owen model to the saltation flux data (Figure 3 and Figure 5). This shows that threshold friction velocity u_{*t} represents different properties of the soil surface in the Owen model and the GP88 model.

5. Conclusions

Three soil surfaces, representing farmland, desert-edge and loess, were tested in a wind-tunnel experiment to examine the dust emission mechanisms. It has been found that:

(1) Flow conditions, saltation bombardment, surface dust content and ground obstacles can all significantly affect dust emission, causing dust emission to change over orders of magnitude;

(2) Dust emission due to aerodynamic entrainment from the natural soil surface is proportional to u_*^{10}, if the supply of free dust is unlimited, as in the initial phase (typically the first 2-3 minutes) of the wind-tunnel runs. This shows that in general, aerodynamic entrainment can be an important (even a dominant) process for dust emission under certain circumstances;

(3) Supply limit is the major reason to restrict dust emission. In nature, dust emission is often supply limited and hence the contribution of aerodynamic entrainment is determined by the renewal of the surface which results in increased availability of free dust for emission;

(4) Surface renewal through saltation and creep of surface particles is the major pathway to ease the supply limit for dust emission. Surface renewal is not only important to the availability of dust for aerodynamic entrainment, but also important to the efficiency of saltation bombardment, η. It is shown that η depends on friction velocity, and the dependency differs for different surfaces reliant on the process of surface renewal;

(5) Existing dust emission schemes do not account for the effects of surface renewal on aerodynamic entrainment and saltation bombardment efficiency, making the accurate prediction of dust emission from different surfaces difficult.

Dust emission is a process driven by fluid motion and restricted by dust supply. The saltation and creep of large particles can generate surface renewal and restore the dust supply. Thus, the contribution of aerodynamic entrainment cannot be overlooked and the processes of supply limitation and surface renewal must be given due attention. Our experiment has shown that aerodynamic entrainment is highly efficient when dust supply is sufficient. Since surface renewal often does not fully liberate the potential of aerodynamic entrainment, dust emission in general can be seen as limited aerodynamic entrainment, and the extent of restriction depends on the degree of surface renewal.

This study does not contradict the earlier perception that saltation plays a fundamentally important role in dust emission, because saltation not only generates bombardment emission and aggregates disintegration, but also provides power for creep and contributes directly or indirectly to surface renewal. What is new in this paper is that we have been able to demonstrate the importance of surface renewal to dust emission.

In addition to the surface renewal by saltation and creep, or dynamic surface renewal, other processes, such as dust deposition and weathering, also contribute to surface renewal. Further experimental observations and theoretical analysis are necessary to establish a general surface renewal model.

Acknowledgments

This work is supported by the State Key Program of National Natural Science Foundation of China (91325203), the National Natural Science Foundation of China (41371034), the Innovative Research Group of the National Natural Science Foundation of China (11421062), the Fundamental Research Funds for the Central Universities (lzujbky-2014-1) and the Hebei Province Department of Education Found (QN2014111).

References

Dong, Z., Sun, H., Zhao, A., WITSEG sampler: a segmented sand sampler for wind tunnel test, Journal of dust research, 23(6), 714-720, 2003.

Gillette, D. A., On the production of soil wind erosion aerosols having the potential for long range transport, Journal de Recherches Atmospheriques, 8, 735-744, 1974.

Gillette, D. A., Fine particulate emissions due to wind erosion, Trans. ASAE, 20, 890-987, 1977.

Gillette, D. A., Environmental factors affecting dust emission by wind erosion, Saharan Dust, 71-94, 1979.

Gillette, D. A., Production of dust that may be carried great distances, Spec. Pap. Geol. Soc. Am., 186, 11-26, 1981

Gillette, D. A., Passi, R., Modeling dust emission caused by wind erosion, J. Geophys. Res., 93, 14233-14242, 1988.

Greeley, R., Iversen, J.D., Wind as a Geological Process on Earth, Mars, Venus, and Titan. New York, Cambridge University Press, 1985.

Houser, C. A., Nickling, W. G., The emission and vertical flux of particulate matter< 10 μm from a disturbed clay - crusted surface, Sedimentology, 48(2): 255-267, 2001.

Huang, N., Gu, Y., Review of the Mechanism of Dust Emission and Deposition, Advances in Earth Science, 11, 1175-1184, 2009.

Kjelgaard, J., Chandler, D., Saxton, K.E., Evidence for direct suspension of loessial soils on the Columbia Plateau. Earth Surface Process. Landforms 29, 221–236, 2004.

Klose, M., and Shao, Y., Stochastic parameterization of dust emission and application to convective atmospheric conditions, Atmos. Chem. Phys., 12, 7309-7320, doi: 10.5194/acp-12-7309-2012., 2012.

Kok, J. F., Parteli, E. J. R., Michaels, T. I., and Karam, D. B., The physics of wind-blown sand and dust, Rep. Prog. Phys., 75, 106901, doi:10.1088/0034-4885/75/10/106901, 2012.

Loosmore, G. A., and Hunt, J. R., Dust resuspension without saltation, J. Geophys. Res., 105, 20663-20671, doi:10.1029/2000JD900271., 2000.

Lu, H., and Shao, Y., A new model for dust emission by saltation bombardment, J. Geophys. Res., 104, 16827-16842, 1999.

Marticorena, B., Bergametti, G., Modelling the atmospheric dust cycle: 1. Design of a soil-derived dust emission scheme, J. Geophys. Res., 100, 16415-16430, 1995.

Macpherson, T., Nickling, W.G., Gillies, J.A., Etyemezian, V., Dust emissions from undisturbed and disturbed supply-limited desert surfaces. Journal of Geophysical Research 113, F02S04, doi:10.1029/2007JF000800, 2008.

Nickling, W. G., McTainsh, G. H., and Leys, J. F., Dust emissions from the Channel Country of western Queensland, Australia, Zeitschrift für Geomorphologie Supplementband, 1-17, 1999.

Owen, R. P., Saltation of uniform grains in air, J. Fluid. Mech., 20, 225-242, 1964.

Rice, M. A., Willetts, B. B., McEwan,I.K., Observations of collisions of saltating grains with a granular bed from high-speed cine-film, Sedimentology, 43, 21-31, 1996a.

Rice, M. A., Willetts, B. B., McEwan, I. K., Wind erosion of crusted soil sediments, Earth Surf. Proc . Landforms, 21, 279-293, 1996b.

Shao, Y., Raupach, M. R., Findlater, P. A., The effect of saltation bombardment on the entrainment of dust by wind, J. Geophys. Res., 98, 12,719-12,726, 1993.

Shao, Y., Raupach, M. R., Leys, J. F., A model for predicting Aeolian sand drift and dust entrainment on scales from paddock to region, Aust. J. Soil. Res., 34,309-342, 1996.

Shao, Y., Lu, H., A simple expression for wind erosion threshold friction velocity, J. Geophys. Res., 105, 22437-22443, 2000.

Shao, Y., A model for mineral dust emission, J. Geophys. Res., 106, 20239-20254, 2001.

Shao, Y., Simplification of a dust emission scheme and comparison with data, J. Geophys. Res., 109, D10202, doi:10.1029/2003JD004372, 2004.

Shao, Y., Physics and modelling of wind erosion, Springer Science & Business Media, 2008.

Shao, Y., Ishizuka, M., Mikami, M., et al., Parameterization of size-resolved dust emission and validation with measurements, J. Geophys. Res., 116, D08203, doi:10.1029/2010JD014527, 2011.

Shao, Y., Wyrwoll, K.-H., Chappell, A., Huang, J., Lin, Z., McTainsh, G. H., Mikami, M., Tanaka, T. Y., Wang, X., Yoon,. S., Dust cycle: an emerging core theme in Earth system science. Aeolian Res. 2, 181–204. doi: 10.1016/j.aeolia.2011.02.001, 2011.

Sweeney, M. R., Mason, J. A.. Mechanisms of dust emission from Pleistocene loess deposits, Nebraska, USA. Journal of Geophysical Research: Earth Surface, 118(3): 1460-1471, 2013.

Újvári, G., Kok, J. F., György V., Kovács, J., The physics of wind-blown loess: Implications for grain size proxy interpretations in Quaternary paleoclimate studies, Earth Science Reviews, doi: 10.1016/j.earscirev.2016.01.006, 2016.

Zhang, J., Shao, Y., and Huang, N., Measurements of dust deposition velocity in a wind-tunnel experiment, Atmos. Chem. Phys., 14, 8869-8882, doi:10.5194/acp-14-8869-2014, 2014.

Atmos. Chem. Phys. Discuss., doi:10.5194/acp-2016-421, 2016
Manuscript under review for journal Atmos. Chem. Phys.
Published: 13 July 2016

Atmospheric Chemistry and Physics Discussions

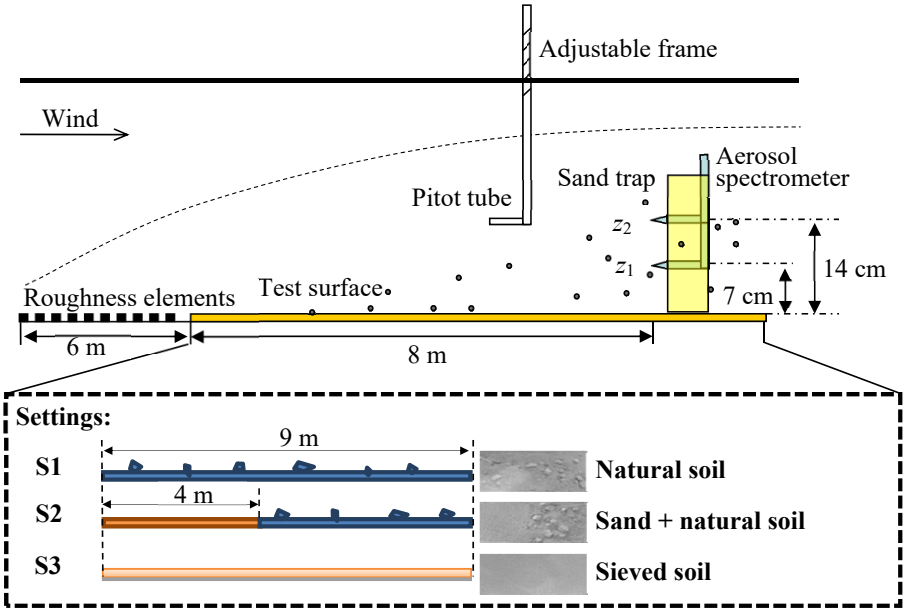

Figure 1: Wind tunnel configuration and simulated soil surfaces.

Atmos. Chem. Phys. Discuss., doi:10.5194/acp-2016-421, 2016
Manuscript under review for journal Atmos. Chem. Phys.
Published: 13 July 2016

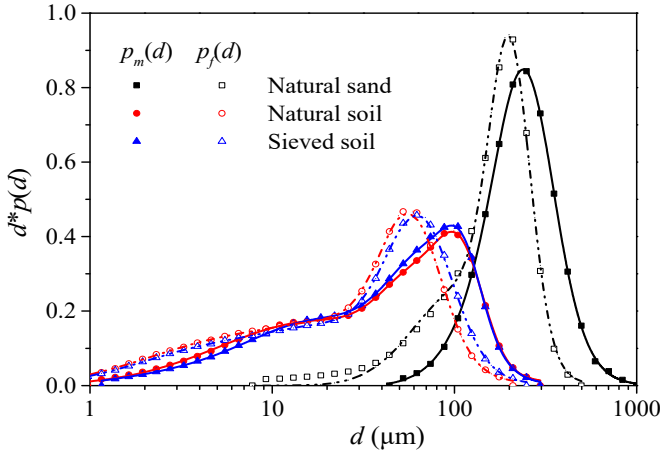

Figure 2: Minimally- and fully-disturbed particle-size distributions of the source materials, namely, the natural sand, natural soil and sieved soil.

Atmos. Chem. Phys. Discuss., doi:10.5194/acp-2016-421, 2016
Manuscript under review for journal Atmos. Chem. Phys.
Published: 13 July 2016

Atmospheric Chemistry and Physics Discussions

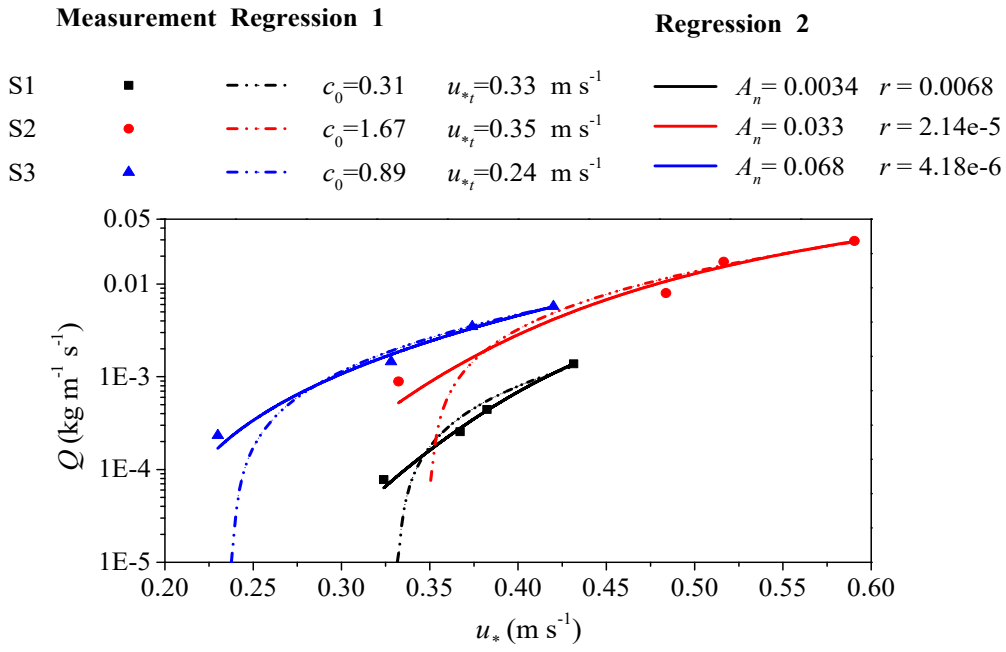

Figure 3: Streamwise saltation flux over the three soil surfaces tested in the wind-tunnel experiment.

Atmos. Chem. Phys. Discuss., doi:10.5194/acp-2016-421, 2016
Manuscript under review for journal Atmos. Chem. Phys.
Published: 13 July 2016

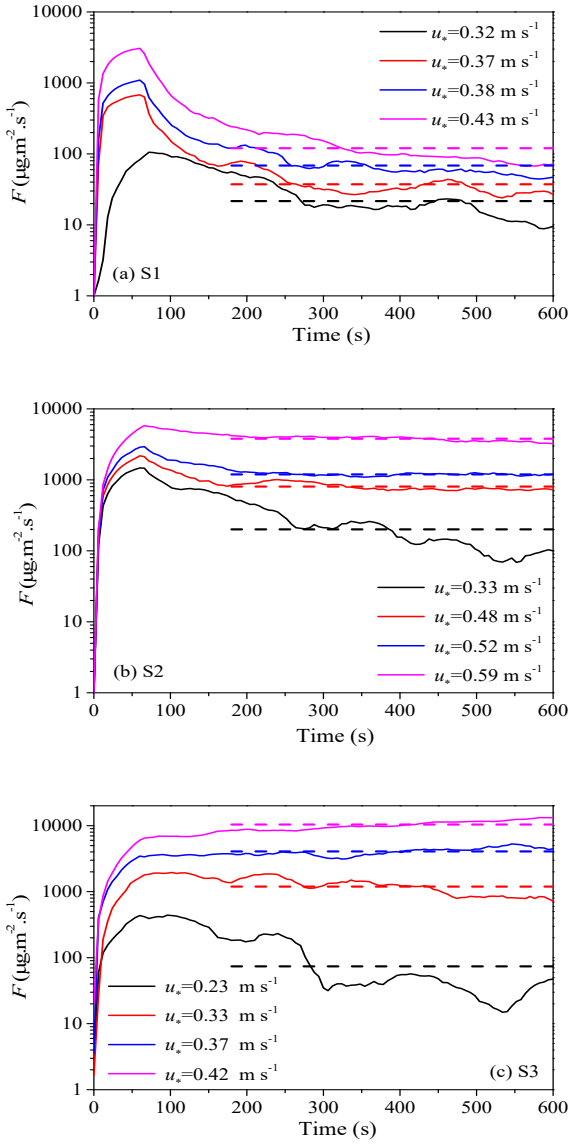

Figure 4: Dust emission flux series over the three surfaces tested in the wind-tunnel experiment.

Atmos. Chem. Phys. Discuss., doi:10.5194/acp-2016-421, 2016
Manuscript under review for journal Atmos. Chem. Phys.
Published: 13 July 2016

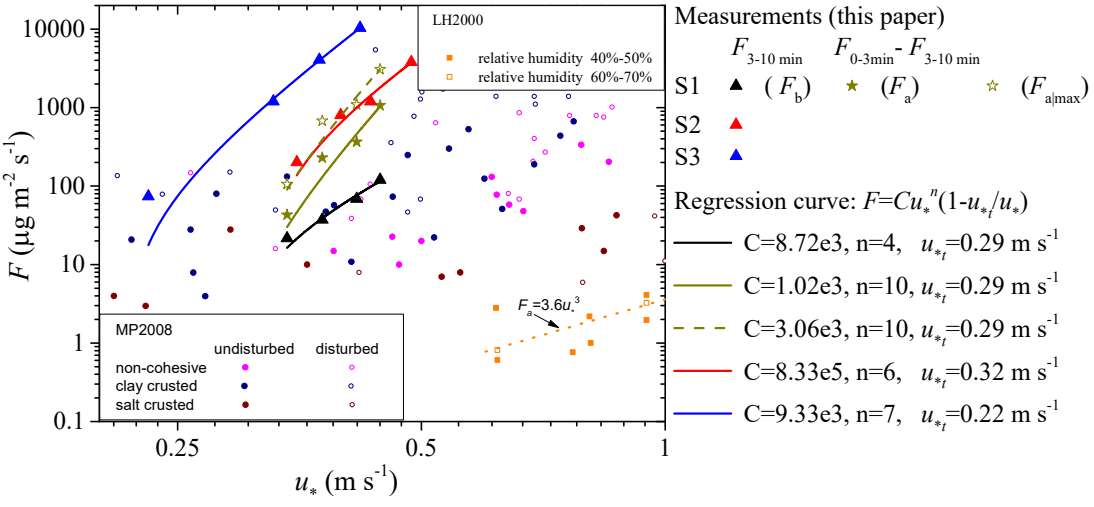

Figure 5: Measured dust emission fluxes over the three different surfaces in the wind-tunnel experiment (triangles), together with the measurements of Loosmore & Hunt (2000, LH2000) and Macpherson et al. (2008, MP2008), labeled as LH2000 and MP2008, as well as the various regression curves.

Atmos. Chem. Phys. Discuss., doi:10.5194/acp-2016-421, 2016
Manuscript under review for journal Atmos. Chem. Phys.
Published: 13 July 2016

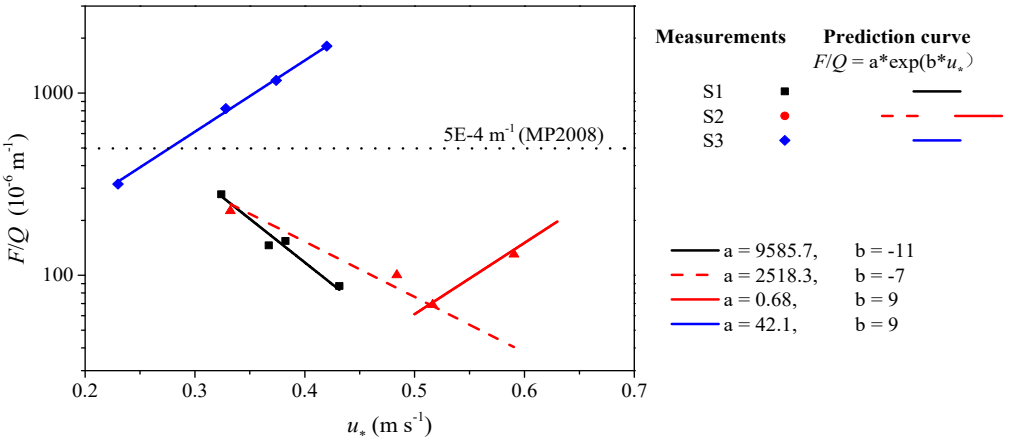

Figure 6: The ratio of dust emission to streamwise saltation flux.

Atmos. Chem. Phys. Discuss., doi:10.5194/acp-2016-421, 2016
Manuscript under review for journal Atmos. Chem. Phys.
Published: 13 July 2016

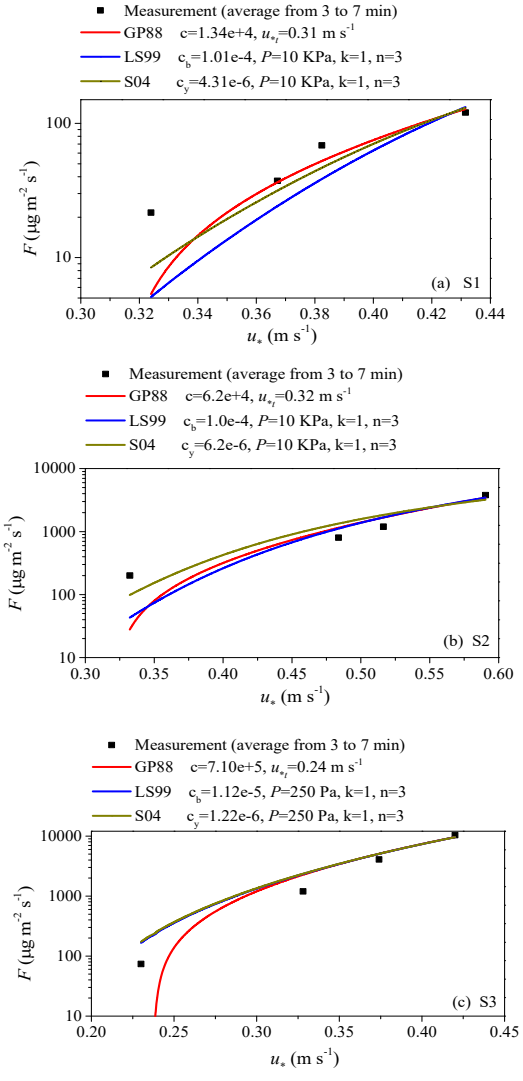

Figure 7: Comparison between measurements and predictions of dust emission fluxes, averaged over the measuring time interval of 3 to 10 min, for the three different surfaces.

Atmos. Chem. Phys. Discuss., doi:10.5194/acp-2016-421, 2016
Manuscript under review for journal Atmos. Chem. Phys.
Published: 13 July 2016

Atmospheric Chemistry and Physics Discussions

Table 1: Runs for the dust-emission experiments.

Surfaces	Runs	Friction Velocity (m s^{-1})	Configuration
S1	1, 2, 3, 4	0.33, 0.48, 0.52, 0.59	Natural soil
S2	5, 6, 7, 8	0.32, 0.37, 0.38, 0.43	Natural soil + natural sand for bombardment
S3	9, 10, 11, 12	0.23, 0.33, 0.37, 0.42	Sieved soil

Atmos. Chem. Phys. Discuss., doi:10.5194/acp-2016-421, 2016
Manuscript under review for journal Atmos. Chem. Phys.
Published: 13 July 2016

Atmospheric Chemistry and Physics Discussions

Table 2: Regression parameters of particle size distribution.

Material		Mode 1			Mode 2			Mode 3			Mode 4		
		W	ln(D)	Σ	W	ln(D)	σ	W	ln(D)	σ	W	ln(D)	σ
Sand	$p_m(d)$	0.471	5.51	0.34	0.529	5.34	0.54						
	$p_f(d)$	0.570	5.31	0.26	0.430	4.70	0.60						
Natural	$p_m(d)$	0.196	4.70	0.29	0.229	4.42	0.43	0.575	2.88	1.23			
Soil	$p_f(d)$	0.357	4.06	0.37	0.314	3.44	0.86	0.329	1.73	1.06			
Sieved Soil	$p_m(d)$	0.109	4.72	0.24	0.372	4.31	0.49	0.488	2.95	1.02	0.031	0.88	0.70
	$p_f(d)$	0.408	4.17	0.41	0.364	3.29	0.92	0.228	1.49	0.94			